OPTICAL DETECTION OF SURFACE DEFECTS IN ORANGES

M. Ruiz Altisent(*), J.L. Pinter and J.M. Otón
ETSI Telecomunicación, Ciudad Universitaria, 28040 Madrid
(*) ETSI Agrónomos, Ciudad Universitaria, 28040 Madrid

ABSTRACT

An optical-based sorting device for oranges is presented. Its design has been based on homogeneity of illumination and detection of the light reflected and scattered by the fruit. Several configurations are studied and compared under semiempirical formulations. A general purpose microprocessor based hardware is proposed. A sorting rate over 10 fruits per second on each channel is achieved.

INTRODUCTION

Fruit sorting has traditionally been a manual process based on external properties, e.g. skin color and sight, fruit shape and remarkable defects. Any of these characteristics, in principle, can be accurately measured and quantified through optical illumination and light detection of the fruit surface.

In the last few years, considerable attention has been paid to non destructive optical assays for quality detection, control and sorting of fruits [1-3]. Several spectrum regions have been proposed (medium and near IR, visible, U.V.) [4] to enhance different aspects or properties of the fruit surfaces and near-surface boundaries.

Our main interest is focused on quality detection and sorting of citrics by optical means. Overall and discrete defects should be separately recognized, and ultimately allow the design of reliable sorting devices at reasonable rates and prices. This paper describes our first results on the field, applied to orange sorting.

EXPERIMENTAL

Valencia oranges were used. Their diameters varied from 7 to 9 cm. approximately. Several series were measured on each experiment, upon criteria of maturity and presence of (colored) defects.

a) Selection of working wavelengths, emitters and detectors.

Visible wavelengths are the obvious choice when dealing with this kind of measurements. Several wavelengths within visible range (488, 514.5 and 632.8 nm) were tested, using Ar^+ and He-Ne lasers. The best discrimination, as expected, was found in the red part of the spectrum. Therefore, He-Ne lasers were used for the other experiments, including detector selection and angular variations. Nevertheless, the laser is substituted by red light-emitting diodes (LEDs) in the actual device (see below).

Detection of scattered and reflected light was attained using light-dependent resistors (LDRs), photodiodes (PDs) and phototransistors (PTs). Reliability and cost criteria were applied to select TIL81 phototransistors working on photodiode mode. These PTs show a good time and wavelength response, and actual measurements only required a simple amplification step. Besides, they show a high directionability which allows the detection of small area defects.

b) Distribution of scattered and reflected light.

One of our first design requirements was to allow 4π detection geometry on the fruit. Obviously, this requires the measure of falling fruits while passing by the detector(s). Synchronization of light emission and detection can be easily achieved; however, it is necessary to optimize spatial distributions of emitters and detectors according to several criteria: i) the illumination of the fruit should be evenly distributed; ii) detectors should cover the whole fruit surface, allowing but minimizing overlapping between areas scanned by different detectors, and iii) detection should be isotropic, i.e. the information ultimately computed should not be affected by rotations of the fruit. First and last conditions point to spherical simmetry distributions of LEDs and PTs.

The next step was to find the angular distribution of the light emerging from the orange upon illumination. As commented above, a He-Ne laser was used to separate the angular dependence of the LED emitters, though they were eventually included in the general calculation. The emergent light can be roughly splitted in reflected and scattered components. Figs. 1 and 2 show the geometries employed for these experiments, while fig. 3 presents some results obtained. When normally incident light is used in fig. 1, and detection angle is varied, scattered light can be selectively measured. Other possibilities of the same setup allow the complete separation between scattered and reflected light, this last one being detected as a sharp peak about the incidence angle.

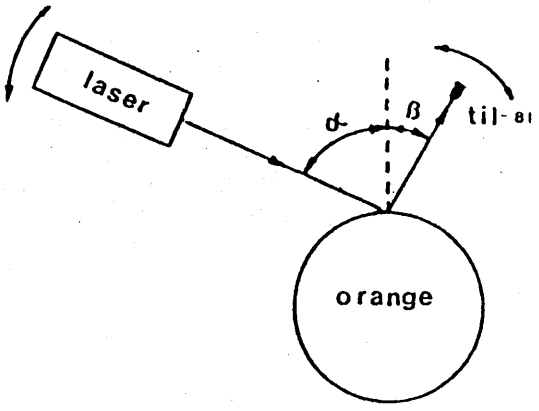

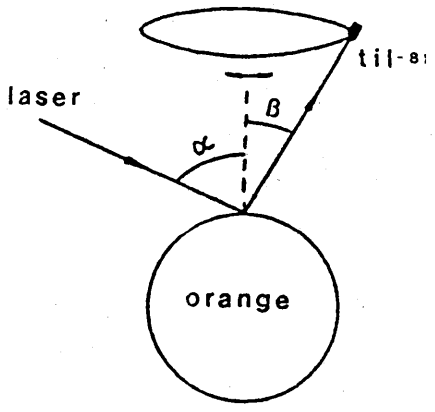

Figs.1 and 2.- Experimental setups

Experimental setup from fig. 2 scans light emerging over conical surfaces at different angles, the incident beam impinging at 30° or 60°. Reflection component is detected as a sudden increase of emitted light for output angles approaching the reflection condition.

MATHEMATICAL SIMULATION OF LIGHT DISTRIBUTION

Light striking a photodetector -for a given setup of emitters- depends on the following: i) angular distribution of LED emission (known, for every PE type); ii) angular distribution of light scattered and reflected by the fruit (measured, experimental); iii) angular distribution of photodetection (known, for a given PT), and iv) distances between emitters, fruits and detectors.

A semiempirical formulation (fig. 3) has been developed to fit experimental results. Light emerging from the fruit can be expressed as a function of

$$\cos\beta + k_1 \left\{ (1 - \sin|\alpha - \beta|) \left[1 - \cos \frac{\alpha \Phi}{\alpha + \beta} \right]^{k_2} \right\}^{(1 + \tan\alpha)}$$

where α is the angle between the incident direction and the normal at the striking point (a spherical surface is assumed); β is the angle between emerging and normal directions, and Φ is the diedric angle between the planes defined by the normal and the incident and emerging beams respectively. The constants are related with the higher or lower "mirror" behavior

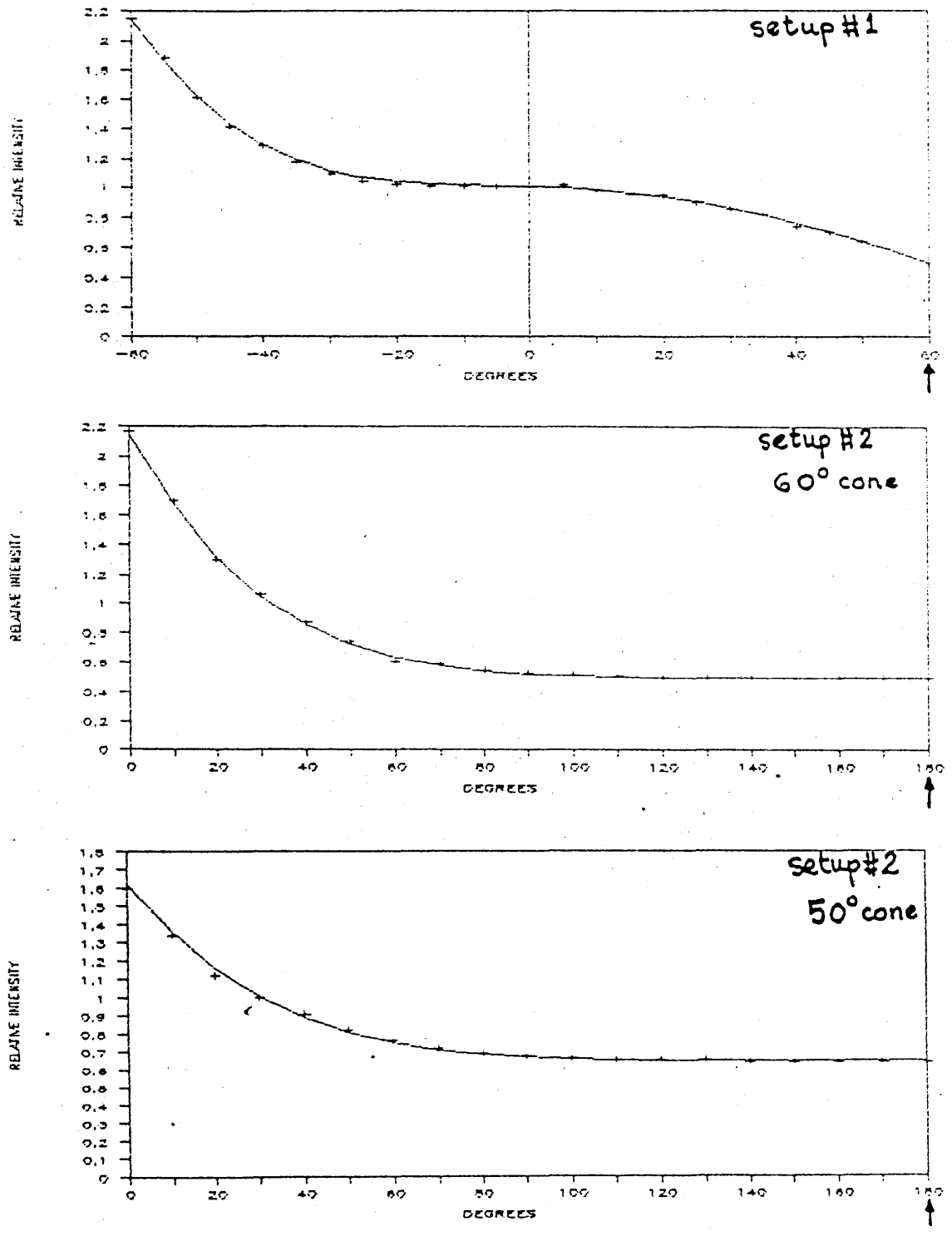

Fig.3.- Light distributions from experimental setups 1 and 2. The x-axis arrow on each figure shows incident light angle. An azimuthal variation is presented on fig.3a. Figs. b and c are precessions of detectors for a 60° incidence; diedric angles are represented.

of the orange surface. Good fittings of experimental data are achieved in our case (fig. 3) for k_1=16 and k_m=1.2.

The overall behavior of the whole PT set has been simulated through a Monte-Carlo method, where at least 25000 points per model where tested, and the final results were plotted as percentages of points yielding different relative light intensities. These results should lead to theoretically optimum geometrical distributions of PEs and PTs, besides practical requirements and constraints.

HARDWARE DESIGN

A general purpose hardware has been prepared. It should have to be accurate and fast enough to adopt logical decisions on accepting or rejecting the fruits (or sorting them into different cathegories) at the maximum expected rate of the device. This rate was primarily established at 10 fruits per second; several channels might be used in parallel to speed up the process.

Under these conditions, the use of a microprocessor is advisable. Actually, initial design and prototypes have been developed on a Sinclair ZX-Spectrum. This is equivalent, in practice, to an easily assembler-programmable Z-80 microprocessor, whose instructions can be modified and adapted as required. This hardware will be substituted by a ROM controlled CPU in the final model.

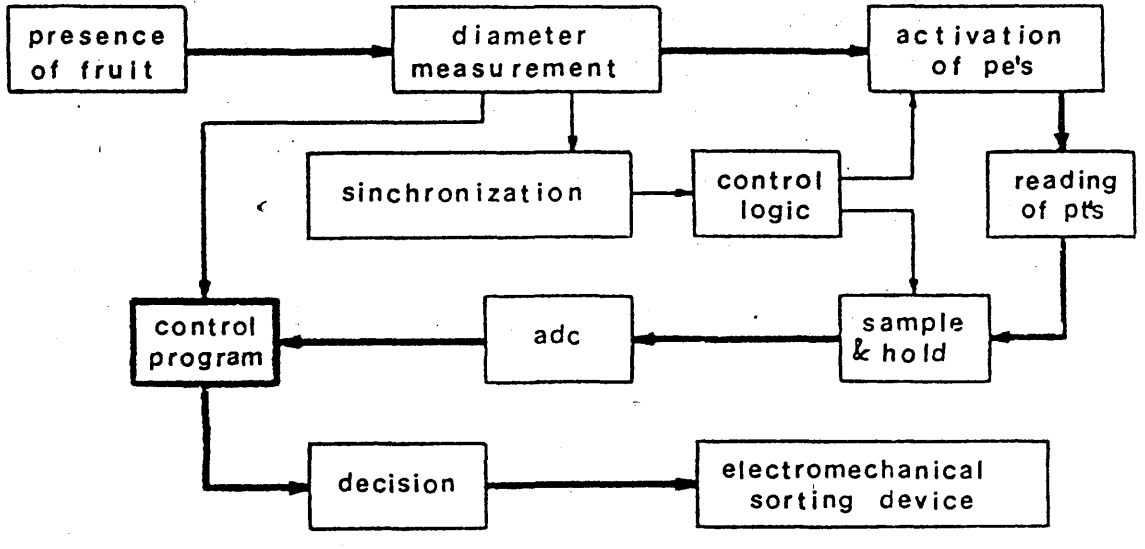

Fig.4.- Hardware diagram. Thick arrows show main logical flux.

Fig. 4 shows the functional diagram of the device. The system receives the following inputs: i) detection of presence of the fruit, from a paired PE/PT device located in the top of the unit. This device is also be used to calculate the fruit diameter as time elapsing for hindered lightpath. ii) Light intensities coming from the fruit surface, as received by the photodetectors. These measurements are hardware-synchronized to the former one, according to fruit diameter, in such a way that PEs are just turned on when the falling fruit is centered in the device, thus allowing simmetrical readings onto the PTs.

System output is the logical acceptance or rejection of the fruit, which eventually activates an electromechanical device. If a different separation criterium is adopted, this device may be substituted by any other kind of sorting unit.

Block diagram of the system logic is presented in Fig. 5. The fruit is detected as an obstacle in lightpath. A counter is activated, and stopped when lightpath is restored. Diameter of the fruit is calculated. A time delay from detection of the fruit to PE activation is also computed according to fruit diameter. Once the time is elapsed, PEs are activated, and PT readings are stored into as many Sample and Hold (S&H) ICs. Thus, the purpose of diameter calculation is two-fold: it allows synchronization of the whole system and, moreover, may be used for calibration purposes, since different fruit diameters yield, of course, different readings on PTs.

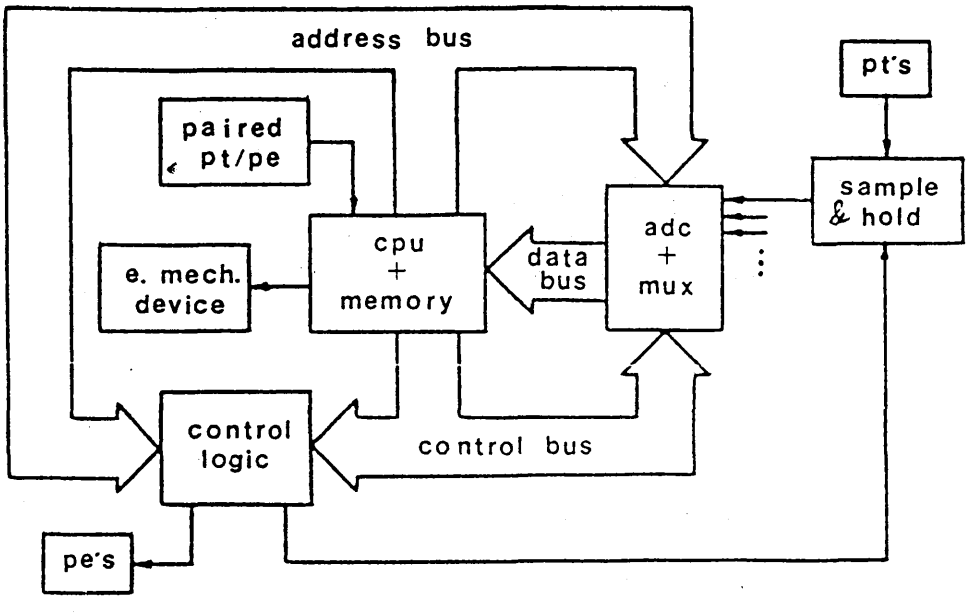

Fig.5.- Hardware block diagram

Next, S&Hs are sequentially read. An analog to digital converter (ADC) is used to translate analogic S&H levels into digital data. A 16-channel multiplexed ADC is employed. Therefore, up to 16 S&Hs (hence, 16 PTs) can be supported.

Finally, information is software-processed, to decide whether the fruit is accepted. This process is fast enough to adopt a decision while the fruit is still falling down. On the other hand, the overall time is under 0.1 s, allowing a fruit rate over 10 fruits per second, as commented above.

RESULTS AND DISCUSSION

a)Geometrical distribution of emitters and detectors

Optimization of PT/PE distributions shall meet simultaneously several (and often opposed) conditions: i) illumination and detection should be homogeneous, thus spherical distribution of a large number of PTs and PEs should be used; however ii) fruits are measured in "free falling" condition, therefore enough room must be reserved along the vertical axis (12 cm circular hole, typically) to allow the fruits passing through; in any case iii) the device diameter cannot be arbitrarily increased, since S/N ratio decreases, and directivity of detection is jeopardized; finally iv) a large number of PTs results in strict hardware requirements, and ultimately may significantly rise the device cost.

An extra point that should be carefully considered is the possibility of light bypass between PEs and PTs. Actually, this undesirable circumstance uses to be a far tighter restriction than the others in many practical cases.

Our proposed configuration has been selected taking into account these constraints, as well as experimental light distributions shown in fig. 3. It is spherically simmetric. Six PE/PT pairs are placed as vertices of an octahedron whose diagonal is 30 cm. The octahedron is tumbled so that two centered triangular "holes" allow input and output of the fruits. Enough room is left for the fruits to pass through. Actually, the limiting fruit size for this configuration is determined for illumination inhomogeneities (see below). A practical limit of 10 cm has been adopted.

In any case, as mentioned above, the general design of the electronics allows eventual modifications either on PT/PE number or their geometries. Up to 16 PTs can be presently supported, the number of PEs being only dependent on power supply limitations. Moreover, sorting rates might be slightly reduced under such conditions.

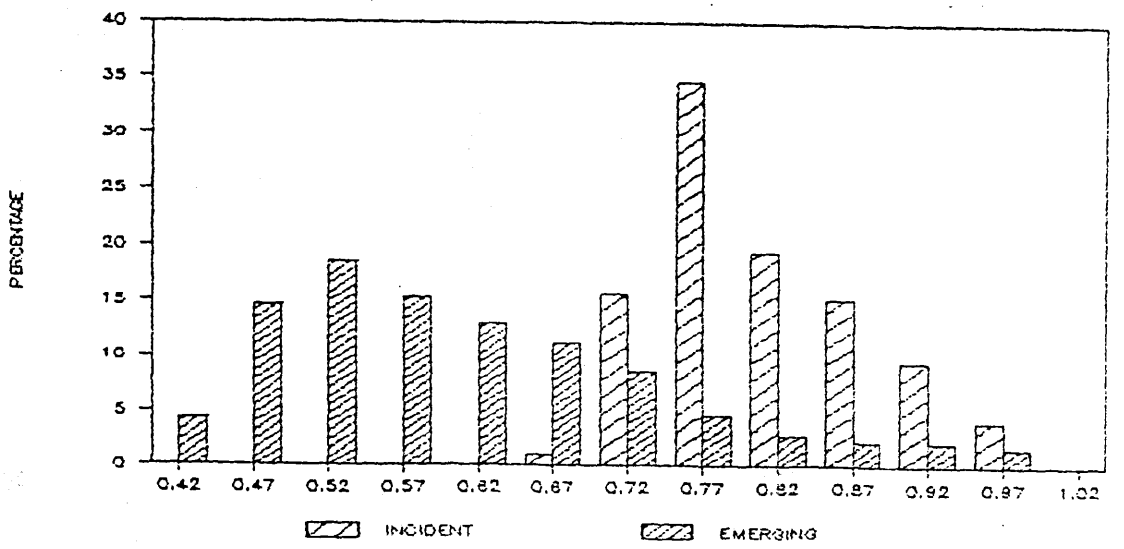

Fig.6.- Monte-Carlo simulation of light distribution onto an 8 cm spherical orange. Six PE/PT pairs are used. See text for details.

b) Light detection

Fig. 6 shows the distributions of emitted and detected light, as seen from the fruit surface. The graph has been obtained through a Monte-Carlo simulation. A fairly homogeneous illumination is observed, whereas a wider range is obtained in detection. This implies that higher sensitivities shall be needed for detection of defects lying on these "low-response" areas.

In practice, a previous calibration of the device is performed, using real acceptable and rejectable fruits, and a lower limit in size is established for the defect to be detected. Among other factors, this limit depends upon the kind of defect and the diameter distribution of the fruits. Diameters are simultaneously measured and their data can be included in the calculations, thus allowing narrower ranges of logical rejections and/or sortings. This last point is presently under study.

REFERENCES

(1) G.G. Dull "Nondestructive evaluation of quality of stored fruits and vegetables" Food Tech. 106, May (1986).

(2) S. Gunasekaran, M.R. Paulsen and G.C. Shove "Optical Methods for Nondestructive Quality Evaluation of Agricultural and Biological Materials" J. Agric. Eng. Res. **32**, 209 (1985).

(3) G.S. Birth "The light scattering properties of foods" J. Food Sci. **43** (3) 915 (1978).

(4) See for example: "Quality detection in foods" J.J. Gaffney ed., Am. Soc. Agric. Eng., St. Joseph, U.S.A. (1976).

(5) J.J. Gaffney "Reflectance properties of citrus fruits" Trans. Am. Soc. Agric. Eng. **16**, 310 (1973).